



# Passive and parallel microfluidic formation of droplet interface bilayers (DIBs) for measurement of leakage of small molecules through artificial phospholipid membranes



Magdalena A. Czekalska, Tomasz S. Kaminski, Karol Makuch, Piotr Garstecki\*

*Institute of Physical Chemistry, Polish Academy of Sciences, Kasprzaka 44/52, 01-224 Warsaw, Poland*

## ARTICLE INFO

### Keywords:

Droplet interface bilayers  
Lipid bilayers  
Droplet microfluidics  
Microfluidic traps  
Alpha-hemolysin

## ABSTRACT

We present a passive microfluidic system for easy and rapid generation of Droplet Interface Bilayer pairs, each formed with two aqueous nanoliter droplets comprising controlled chemical composition. The system allows for rapid screening to quantify leakage of small molecules through artificial phospholipid bilayers. The droplets are generated, diluted and stored in-situ on the microfluidic chip. Our device comprises microfluidic Meter&Store (M&S) modules – hydrodynamic traps, which enable hard-wired operations on small – ca. 9 nL in volume – aqueous droplets including splitting, merging and derailing the droplets to side storage wells. Consequently, the droplets are locked and positioned next to each other and form bilayers at the point of contact between the nanoliter aqueous compartments. Additionally, a set of trap modules provides the possibility for in situ preparation of dilutions of a sample. We demonstrated the basic capacity of the trap-based system for formation of an array of 12 (controllably different) lipid bilayers in less than 5 min. Thanks to the small volumes of the droplets, the system is capable for monitoring the transport across the artificial membrane within a relatively short interval – opening the possibility to use dyes and alleviating the difficulty of parallel electrophysiological measurements. We use this functionality to prepare on-chip dilutions of small molecules and determine their permeation rates through the bilayer. Finally, we used the M&S system and calcium sensitive dyes to quantify the ion flux through the model  $\alpha$ -hemolysin ( $\alpha$ HL) nanopores.

## 1. Introduction

We report a droplet microfluidic system for the rapid, parallel and facile formation of arrays of model lipid bilayers. The method is based on the technology of hydrodynamic traps – microfluidic geometries that allow for passive procedures on aqueous plugs dispersed in oil phase – that we here demonstrate operational for droplets of volumes as small as 9 nL.

Numerous studies focus on phenomena occurring at the artificial lipid bilayers [1–4]. Systems allowing for facile and quick formation of stable biomimetic bilayers are in high demand. In recent years a number of microsystems were proposed for the generation of artificial membranes. One of the approaches is based on the self-organization of phospholipid molecules into a monolayer at the interface of aqueous droplets submerged in oil. The operation of bringing together two droplets results in formation of a lipid bilayer at the interface between them [5–7]. The control over the content and position of an individual droplet and the ability to generate multiple such droplets are the main

motivation for the use of Droplet Interface Bilayers (DIBs). In this paper, we present an easy to operate tool that allows to exploit the benefits of the DIBs - a microfluidic system for efficient formation of arrays of lipid membranes, with a gradation of concentration of the active compounds in compartments separated by the membranes.

One of the simplest and the most efficient methods to study the transport processes in the lipid membrane is the measurement of the changes in concentration of a given compound in compartments separated by the bilayer. Determination of the rate of passive permeation through the artificial bilayer is one of the methods in the assessment of transcellular transport of a given chemical compound. Microfluidics provides the possibility to repeatedly form nanometer-thick stable bilayers, and to monitor the interior of the aqueous microcompartments. However, there are just a few examples of microfluidic systems based on fluorescence read-out designed for measurements of passive permeation of small molecules through the lipid bilayer [8–13].

Another reason for formation of biomimetic artificial lipid bilayers is studying of the communication between cells and environment which

\* Corresponding author.

E-mail address: [garst@ichf.edu.pl](mailto:garst@ichf.edu.pl) (P. Garstecki).

<https://doi.org/10.1016/j.snb.2019.01.143>

Received 26 September 2018; Received in revised form 30 December 2018; Accepted 28 January 2019

Available online 29 January 2019

0925-4005/ © 2019 Elsevier B.V. All rights reserved.

is a complicated process, facilitated by membrane proteins' machinery. So far, there are a few demonstrations, in which activity of membrane proteins was investigated via fluorescence measurement in microfluidic systems. Ota et al. [14] presented a PDMS device with an array of microchambers – recesses of walls in parallel channels – for measurements of flux of calcein dye through  $\alpha$ -hemolysin nanopores. By alternately flushing the channels with aqueous sample and with an immiscible organic solvent containing the phospholipid, bilayers were formed between the microchambers and the main channels. Monitoring of diffusion of calcium ions through  $\alpha$ -hemolysin nanopores was demonstrated as a proof-of-concept experiment by Castell et al. [15] who presented a method of deposition of an aqueous droplet on the surface of planar hydrogel for formation of an array of bilayers. Fluo-8 dye was used to detect the transport of  $\text{Ca}^{2+}$  cations. Additionally, authors measured the inhibition of ionic flux through  $\alpha$ HL by gamma-cyclodextrin. Tonooka et al [16]. constructed a device, in which an array of hemispherical picoliter droplets is brought into contact with one larger droplet. Silicon wafers containing thousands of cavities were used to generate membranes either from spread Giant Unilamellar Vesicles [17,18] or from lipid solutions in organic phase [19,20]. Recently a non-complicated, passive system for generation of networks of droplets interconnected with lipid bilayers was proposed previously [21]. Although the device explores standard microfluidic techniques (soft lithography) for fabrication of trapping structures, the contact area between the droplets varied (possibly due to the swelling of PDMS) preventing a quantitative analysis of transport between the compartments. In addition, the capability of preparing dilutions on chip was not met.

So far the proposed systems were limited by the high degree of complexity in terms of the fabrication and equipment needed for the operation of the device e.g. piezo actuated nano-injection systems for dispensing of nanolitre droplets. The challenge lies in the construction of simple-to-operate system that could be operated in a conventional biochemistry laboratory, without specialized infrastructure and without any expertise in microfluidics at hand [22]. A perfect system should allow for efficient formation of lipid bilayers and for examination of various concentrations of a tested compound in parallel.

Here we demonstrate such a method – a microfluidic device that allows for rapid, facile and parallel generation of up to 12 lipid bilayers with all the liquid samples simply delivered from a syringe pump. The processing of a sample on a chip – diluting, partitioning into droplets and formation of pairs of droplets – is hard-wired in the hydrodynamic traps for passive handling of fluids. We demonstrate the efficient formation of lipid bilayers at the interface of droplets and monitor the passive permeation of fluorescent dye from the donor to the acceptor droplet. We also show the quantification of transport rate of calcium ions through  $\alpha$ -hemolysin nanopores as a function of concentration of the channel-protein.

## 2. Experimental

### 2.1. Materials

For the continuous phase, DPhPC (Avanti Polar Lipids, USA) was dissolved in 90% v/v hexadecane (Alfa Aesar, Germany), 10% v/v AR20 silicone oil (Sigma Aldrich, Germany) at 0.5 mg/mL and DOPC (Avanti Polar Lipids, USA) was dissolved in 92.5% v/v hexadecane, 7.5% v/v AR20 at 2.5 mg/mL. For permeation experiments, the aqueous phase comprised of 150 mM KCl (Chempur, Poland), 10 mM HEPES (Sigma-Aldrich, Germany) for empty droplets and 100  $\mu$ M fluorescein isothiocyanate (FITC, Sigma Aldrich, Germany), 150 mM KCl, 10 mM HEPES for fluorescent droplets. In the experiments of calcium ions transport through hemolysin pores, we used solution of 100 mM  $\text{CaCl}_2$  (Chempur, Poland), 10 mM HEPES and solution of 600 nM  $\alpha$ -hemolysin (Sigma-Aldrich, Germany), 10  $\mu$ M Fluo-8H (AAT Bioquest, USA), 10 mM HEPES, 0.34 mM EDTA (Sigma-Aldrich,

Germany). In the experiment of testing of preparations of dilutions, we used 20  $\mu$ M Rhodamine 110 chloride (Sigma-Aldrich, Germany) diluted in 150 mM KCl, 10 mM HEPES.

### 2.2. Preparation and operation of microfluidic devices

Microfluidic devices were prepared by micro milling of 5-mm- and 2-mm-thick polycarbonate plates (Makrolon, Covestro, Germany) and bonding them in a hydraulic press at a temperature of 130 °C for 30 min. In the SI we have included some advices for successful and precise fabrication of polycarbonate chips via micromilling. The surface of the channels was modified with Aquapel (PPG Industries, USA) in the experiments involving the use of  $\alpha$ -hemolysin, by flushing the channels twice in 30 min time period, and subsequent overnight incubation in 75 °C in order to completely evaporate modification agent. This step was critical, as in the course of experiments we noticed that residues of Aquapel might influence the activity of Fluo-8 dye. The continuous phase comprising the mixture of hexadecane and silicone oil AR20 supplemented with lipids, as well as aqueous samples, were supplied to the chip from gastight glass syringes (series 1700 RN, Hamilton, USA) connected to the chip through PTFE tubing. The flow of fluids was controlled by set of Nemesys syringe pumps (Cetoni, Germany). The outlet tubing was terminated with a PTFE miniature 2-way stopcocks (Bola Bohlender, Germany).

### 2.3. Fluorescent microscopy and data analysis

Fluorescence images were taken with A1-R Eclipse Ti confocal microscope (Nikon, Japan) with using an objective 10 $\times$ . We used excitations/emission wavelengths of 488/500–550 nm to record fluorescence signal from FITC and Fluo-8H dyes. The images from experiments were analyzed in NIS-Elements AR software (Nikon, Japan).

## 3. Results and discussion

### 3.1. Results

#### 3.1.1. Operation of a single M&S module

The most important functional module of the system is the Meter&Store unit [23]. For the purpose of measurements of molecular transport through lipid bilayers, we scaled down the dimensions of the M&S module to operate on droplets with volume of less than 10 nL – ca. 50 times smaller than in the system presented earlier by Derzsi et al. [23]. A single module consists of a metering trap and adjacent storage well (Fig. 1a).

The metering trap comprises a step – barrier that perpendicularly obstructs the channel and a set of bypasses – a widening of the channel milled to 33% of its normal depth. When an aqueous plug longer than the trap encounters the barrier the rear of the droplet blocks the entrance for the continuous phase to the bypasses. As a result, the droplet is being pushed through the barrier until the rear of the droplet aligns with the entrance to the bypasses and the oil starts to flow around the droplet. Then, the droplet is split at the barrier into two portions – one part of a well-defined volume locked in the trap and the remaining part being pushed further into the main channel. When the flow of continuous phase is stopped, the droplet locked in the metering trap begins to spontaneously flow back to the storage well. This spontaneous movement of the droplet is achieved passively with capillary forces that pull the droplet out of the converging metering trap.

#### 3.1.2. Geometry of the microfluidic chip

The whole device consists of microfluidic T-junctions for dosing of aqueous samples and a set of 9 or 12 Meter&Store modules (Fig. 1b and c). For the experiments that did not require dilutions of sample, we rather use a simplified design of the device consisting of 9 traps, than the more elaborated one, dedicated for preparing gradients of

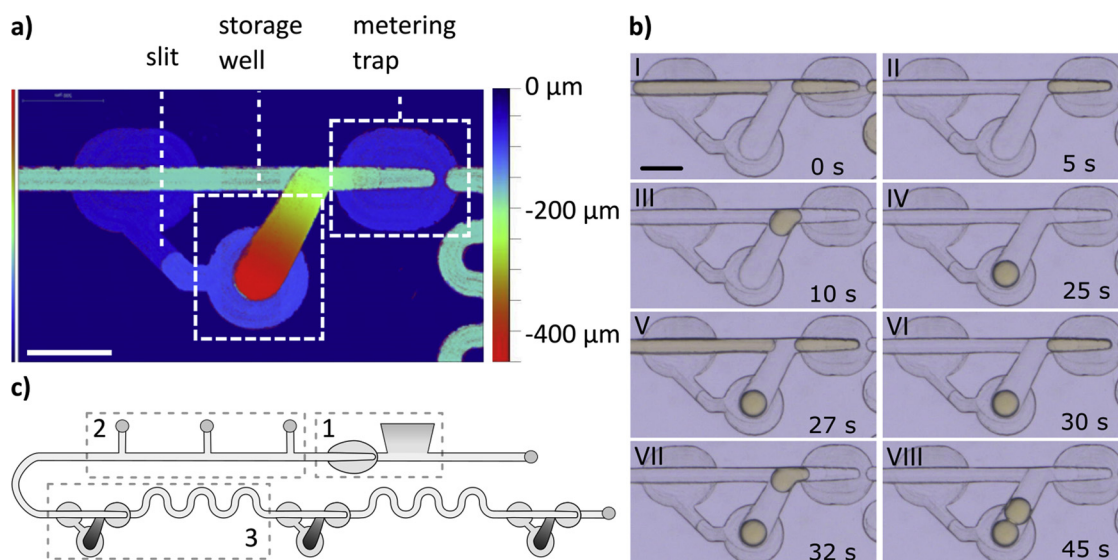


**Fig. 1.** Design and operation of microfluidic device for sequential generation of DIBs. a) Profilometry scans (recorded by Bruker ContourGT-K, USA) depicting the architecture of the microfluidic trap. The trap consists of a part for metering of  $\sim 9$  nL droplets, a widening and deepening storage well and a slit for equalizing of the flow of oil. b) Formation of DIBs in a single Meter&Store module: an aqueous sample is metered into portions (I) and after the flow of oil is halted (II) the droplet is passively dragged to the bottom of the well (III–IV). Metering of a second type of aqueous sample is performed (V–VI), and the droplet is directed to the storage well (VII) to contact the already stored droplet and form a lipid bilayer at their interface (VIII). Scale bars in a) and b) are  $500 \mu\text{m}$ . c) Scheme of the device: “1” – metering module dedicated for operations in dilution mode, “2” – inlets for aqueous samples, “3” – Meter&Store module with serpentine channel for mixing of droplets content.

chemicals. An additional metering trap and storage well is added for precise dosing of a sample in the dilution module. The width and depth of the channels is  $160 \mu\text{m}$ , except for dimensions of selected details (e.g. barrier and bypasses) in trap modules. The capacity of the whole 12-traps device is approximately  $10 \mu\text{l}$ , and small dimensions of channels significantly reduce the total volume (to ca.  $30 \mu\text{l}$ ) of oil required for the execution of the whole protocol on the chip. The sequence of operations of trapping, merging, diluting, i.e. all steps required to prepare the set of up to 12 pairs of droplets with a serial dilution of an agent in one of the droplets in the pairs, requires the flow of oil at the rate between 0.1 and 0.3 ml/h.

### 3.1.3. Formation of DIBs

We are able to form lipid bilayers at the interface of a pair of droplets locked in the storage wells. In the first step, we fill the chip with continuous phase. Then we deposit first type of aqueous sample, and push it through the chip and aliquot into droplets of predefined (by the geometry of the microfluidic modules) volumes ( $8.7 \pm 0.5$  nL) in the successive traps. After the flow of oil is halted, the droplets formed in the metering traps are autonomously derailed to the adjacent storage wells by the action of capillary forces. Then, the other type of aqueous sample is introduced onto chip and flows through the set of metering traps, and is being aliquoted into portions of liquid. These, again, after stopping the flow of oil, spontaneously move into the storage wells. In the storage wells the two droplets meet and touch each other (Fig. 1b). As both of the droplets are covered with a monolayer of 1,2-diphytanoyl-*sn*-glycero-3-phosphocholine (DPhPC) or 1,2-dioleoyl-*sn*-glycero-3-phosphocholine (DOPC) lipids, they do not coalesce, but rather form a lipid bilayer at their interface. The successful formation of a bilayer is confirmed with the characteristic change in the reflection of light at the interface of droplets. The removal of droplets from storage wells is executed by applying the flow of oil at rate higher than 5 ml/h.

### 3.1.4. Permeation of fluorescein through lipid bilayers

We determine the permeation coefficients for FITC molecules across DOPC bilayers by analysis of changes of concentration over time. For this purpose, we generate a collection of 9 pairs of droplets comprising

‘acceptor’ (150 mM KCl, 10 mM HEPES) and ‘donor’ (100  $\mu\text{M}$  FITC, 150 mM KCl, 10 mM HEPES) compartments (Fig. 2a). We measured the intensity of fluorescence of each droplet every 5 min over a period of 2 h and plotted the changes in the concentration of fluorescein versus time (Fig. 2b).

In the experiment, the concentration of fluorescein within each of the droplet is homogeneous. The diffusion coefficient of fluorescein in water is  $D = 0.49 \cdot 10^{-9} \text{m}^2/\text{s}$  [24]. Therefore, any inhomogeneities in the droplet of radius  $r = 128 \mu\text{m}$  are relaxed over a characteristic time  $t = (r^2)/D$  which is 33 s. In order to determine the coefficient of diffusion through membrane we assume that the rate of permeation of fluorescein is proportional to the difference between concentration in donor and acceptor,  $c(t) \equiv c_d(t) - c_a(t)$ . Thus, time-dependent evolution of the concentration is described by the following equation:

$$V \frac{dc(t)}{dt} = -2Skc(t), \quad (1)$$

where  $k$  is the permeability coefficient of the membrane,  $V = V_a = V_b$  is the volume of the donor and acceptor droplets and  $S = 10\,250 \mu\text{m}^2$  is the surface area of the membrane estimated from the image of the droplets (see ESI for details). Solution of the above equation leads to exponential decay of the difference in concentration with time,  $c(t) = c_0 e^{-2Sk t/V}$  and, equivalently, the logarithm of concentration difference  $\log c(t)/c_0$  is proportional to time as follows:

$$-\log \frac{c(t)}{c_0} = 2 \frac{Sk}{V} t. \quad (2)$$

Plot depicting the increase of logarithm of averaged difference of concentration over a time is shown in Fig. 2c. We fit Eq. (2) to the experimental data from Fig. 2c. We obtain the following permeability coefficient  $k = 5.39 \times 10^{-8} \text{m/s}$ .

### 3.1.5. Dilutions of protein sample on-chip

We also used the very same Meter&Store system to demonstrate that it can be used for generation of dilutions of the sample. Prior to the execution of experiments on protein samples we have evaluated the performance of the dilutor using Rhodamine 110 dye. Fig. 3a shows the pairs of droplets in which one droplet contains consecutively diluted

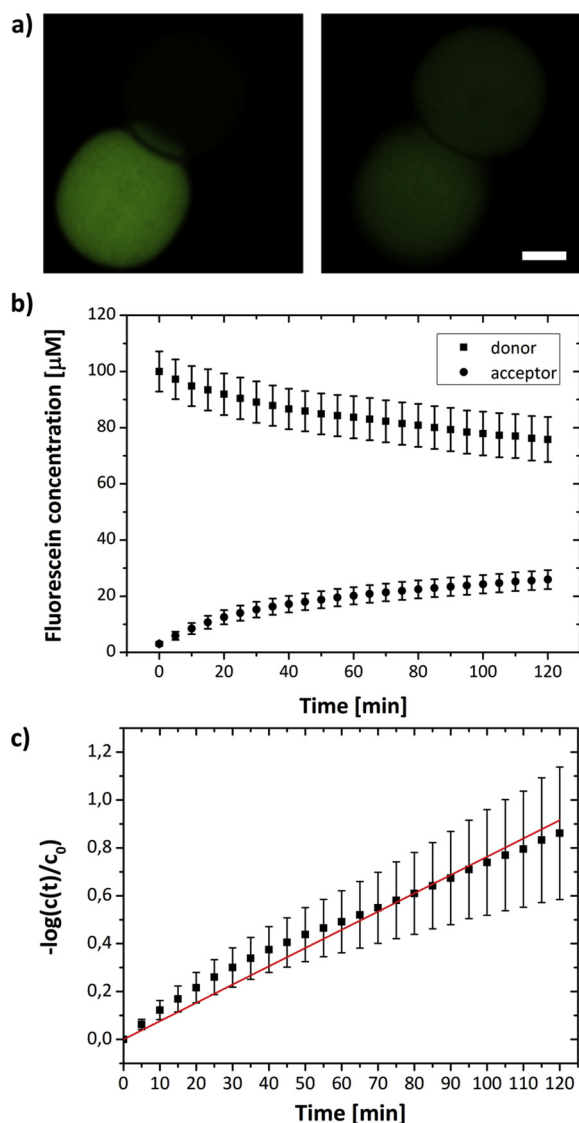


**Fig. 2.** Permeation of fluorescein through lipid bilayers. a) Snapshots depicting the pair of droplets before the measurement (left panel) and after 120 min of incubation (right panel). The donor droplet was 100 μM FITC, 150 mM KCl, 10 mM HEPES and the acceptor droplet was 150 mM KCl, 10 mM HEPES. Scale bar is 100 μm. b) Variation of fluorescein concentrations measured within droplets in time ( $n = 9$ ). c) The logarithm of the concentration difference between two droplets in pair is linear in time (data averaged over 9 pairs of droplets).

dye. The assembly of droplets was prepared as follows:

- i first the plug of 20 μM rhodamine is aspirated with a reverse flow of oil from one of the inlets to the module 1 (Fig. 1c) for a precise metering,
- ii then the flow of oil is set to the dosing mode and in the same time droplets of pure buffer are generated at one of the T-junctions,
- iii next we generate the flow of oil which moves the droplets of a buffer immediately followed by a droplet of undiluted rhodamine to the set of Meter&Store traps,
- iv the sample is diluted in the subsequent traps and, after switching off the flow of oil, the droplets comprising dilution series are directed to the storage wells,
- v in the next step we generate a sequence of droplets of a buffer and split them into 12 droplets that flow back to the wells where they form bilayers at the interface with already stored droplets (see Figs.

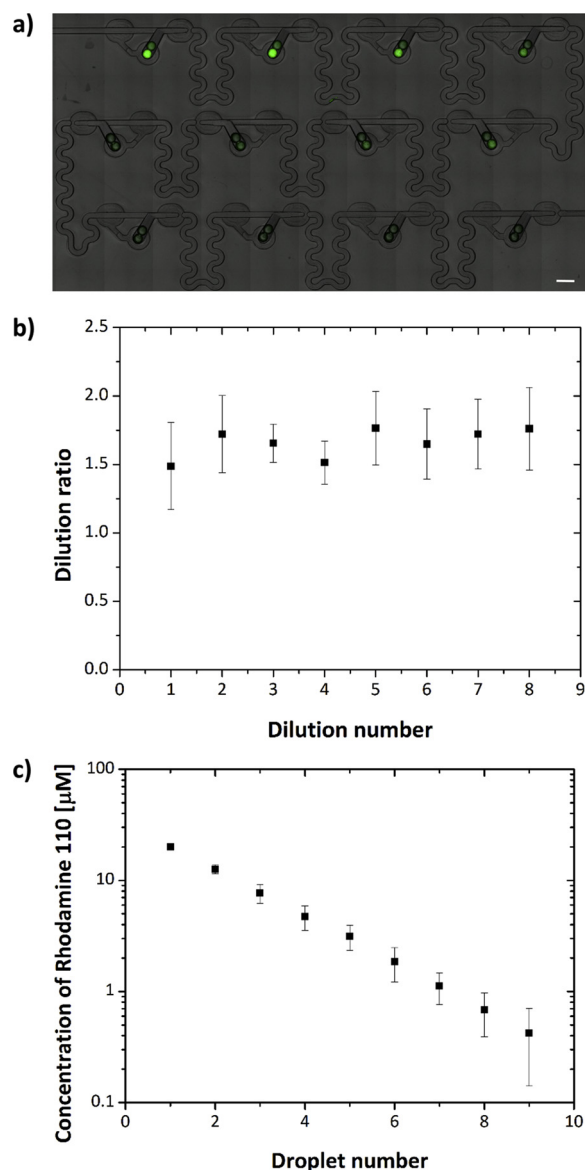


**Fig. 3.** Dilutions on a chip. a) Rhodamine 110 (20 μM) was diluted in 12 subsequent traps. The droplets were stored in wells and exposed to droplets of buffer. b) The dilution ratio between the following trap modules calculated from the intensity of fluorescence,  $n = 7$ . c) From the intensity of droplets, the concentration of rhodamine was calculated,  $n = 7$ . The level of fluorescent signal in the last three droplets (no. 10–12) was below the sensitivity of the detector and could not be included in this plot.

S3–S6 and Supplementary videos for more details).

The experiment was repeated 7 times. We have determined the dilution ratio equal to  $1.6 \pm 0.2$  between following traps based on the comparison of the fluorescence intensity inside the droplets (Fig. 3b). Further the intensity was calculated into the concentration of rhodamine and plotted on the log scale (Fig. 3c).

We performed measurements of activity of  $\alpha$ HL protein in bilayers formed by DPhPC lipids (dissolved at 0.5 mg/ml in oil).  $\alpha$ HL pores penetrate lipid bilayers by forming water-filled channels in its structure. The channels non-selectively and passively allow small molecules, including calcium ions, through their pore. We monitored the increase of fluorescence in droplets containing the calcium sensitive Fluo-8 dye. We attribute the increase of fluorescence to the transport of calcium ions through the  $\alpha$ HL channels in bilayers. In the control experiment, we did not observe any leakage of calcium ions when no  $\alpha$ HL pores

were present (Fig. S9). In the first step, we meter a portion of concentrated stock solution of protein (600 nM  $\alpha$ HL, 150 mM KCl, 10 mM HEPES, 250  $\mu$ M Fluo-8H, 0.34 mM EDTA) in a *module 1* (Fig. 1c) and prepare sequence of aqueous plugs with buffer (150 mM KCl, 10 mM HEPES, 250  $\mu$ M Fluo-8H, 0.34 mM EDTA) at one of the T-junctions (*module 2*, Fig. 1c). *Module 1* consists of a metering trap and storage well, that have larger volumes than the single Meter&Store unit (*module 3*, Fig. 1c). We flow the buffer (followed by the protein plug) through the Meter&Store units. Buffer is metered into predefined volumes and, as we do not stop the flow of oil, the droplets do not flow back into the storage well. Instead, they are immediately merged with a following droplet containing  $\alpha$ HL. The plug, which is pushed out as a result of merging of buffer with the concentrated protein, has a volume equal to the initial volume of protein sample. Mixing of the content of droplet takes part by convection in the winding channel, before the droplet enters the following Meter&Store unit for further dilution. This way, we prepare droplets with gradually decreasing concentration of nanopores, and after we switch the flow of oil off, they are passively (i.e. by capillary forces) directed to the bottom of the side storage chambers.

Next, we generate a sequence of droplets containing calcium ions (100 mM  $\text{CaCl}_2$ , 10 mM HEPES) at one of the T-junctions (*module 2*, Fig. 1c). The plugs are metered in the 12 Meter&Store units and stored in the wells after switching the flow of oil off. We measure the leakage of calcium ions depending on the number of protein pores present in the bilayer and plot it versus time (Fig. 4). The more nanopores are present in the membrane, the faster is the increase of fluorescent signal coming from the excitation of dye with the calcium molecules. At some point the curve reaches a plateau meaning that the number of calcium ions exceeds the number of available Fluo-8 molecules. The model used to describe the diffusion of fluorescein molecules in Section 3.1.4. is modified to calculate a permeability coefficient. Based on the obtained curves and literature data on nanopore dimensions and diffusion of calcium ions in a protein channel, we derive the permeability coefficients of membranes and the equation for the number of protein pores at any time (see SI for the full description of the model and calculations). As an example, we estimate that for the concentration of 600 nM of  $\alpha$ HL, after 40 min of measurement,  $1.2 \times 10^4$  pores are present in the bilayer.

### 3.2. Discussion

We demonstrate a simple-to-use microfluidic device which opens the possibility of generation of multiple lipid bilayers from very small samples of the lipid and the protein. In recent years number of papers

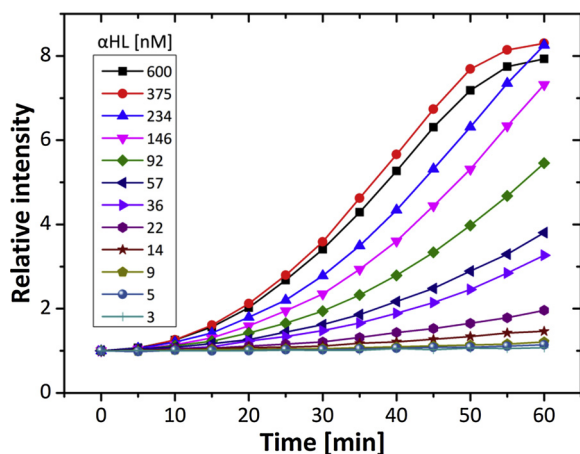


Fig. 4. Transport of calcium ions through  $\alpha$ HL nanopores - dilutions of protein sample on-chip. An exemplary plot depicts the mean pixel intensity of the droplet area observed from excitation of Fluo-8 over time. The concentration of  $\alpha$ HL nanopores was calculated using the value of dilution ratio equal to 1.6.

reported systems dedicated for efficient formation of miniaturized bilayers, yet only a few of them represented a format that would be easy to fabricate and operate. We fulfil these demands by utilizing microfluidic modules for development of a device in which formation of bilayers will require neither a skilled operator nor sophisticated equipment. Up to 12 bilayers are formed at the interface of droplets, which are metered in special microfluidic modules from a random sequence of liquid plugs. The volumes of droplets, and hence the area of the bilayers formed between 2 droplets, are uniform. We did not observe malformation of bilayers resulting from e.g. coalescence events. We confirm that formed membranes are functional lipid bilayers with experiments showing the passive transport of small fluorescent molecules and with insertion of protein molecules into the bilayer.

The number of droplet pairs and bilayers can be further increased by parallelization of droplet microfluidic modules [25], realistically by the factor of 8, resulting in the number of 96 droplet pairs, that could be imaged with a motorized microscopes or automated imaging plate readers. However, it would probably require the use of more precise CNC micromilling machine, careful design and adjustment of channel resistances in parallel dilution modules (e.g. by implementation of flow resistors) and finally the need of smart sample deposition strategy e.g. similar to 3D-printed lids sealing the inlet for the sample [26]. It is worth to note that the down-scaling of structures of microfluidic Meter & Store traps [23], was not trivial in terms of both the difficulty of microfabrication and tuning of the aspect ratios of the structures for the particular choice of fluids and the scale of the chambers. Especially, the dimensions of metering traps, such as the depth of bypasses, the height of the barrier and the length of the trap needed to be optimized – a task that required ca. 10 iterations. The lipid solution that we use has a very low ( $< 1$  mN/m) [27] interfacial tension with water – this is a much lower value in comparison to fluorocarbon oils (reported values 3–14 mN/m) [28–30] used in previous study published by Derzsi et al. Low surface tension favours formation of satellite droplets at the steps and barriers in the traps. We needed to carefully choose the dimensions and aspect ratios of the traps to avoid this unwanted process of generation of small satellite droplets. In particular, we decreased of the height of the bypass in the metering trap and adjusted the height of the bypasses and barriers located around the storage well and made them deeper – to 50% of the depth of the main channel (previously the depth of this bypass was 33% of the main channel). This change was necessary to speed up the derailing of the droplet from the metering trap to the well.

The hydrodynamic trapping of droplets for formation of lipid bilayers has been shown by others [21,31–33], yet, here, for the first time, the Meter&Store system combines the ability of facile preparing on-chip dilutions of a sample with passive positioning of droplets. This feature enables rapid screening of various concentrations of proteins. However the precision of the performance of the dilutor is lower than for the original design (mean RSD 14% and 4%, respectively) [23], which can be attributed to the smaller volume of droplets and the presence of phospholipids in the continuous phase. Droplets have to merge during dilution in the metering trap but later they have to remain unfused and separated by the bilayer in the side well of the trap. The merging during dilution is facilitated by squeezing of droplets and then pulling them apart – this phenomenon was previously described by Bremond et al. [34]. However, the reproducibility and precision of dilution might be higher for decreased phospholipid concentration in the oil – an approach that cannot be applied in the current design due to the need of formation of bilayer in the side well in the next step of the protocol. However, in the future applications one can consider sequential using of two supplies of oil. First low concentration of surfactant can be injected for metering of buffer droplets and for the dilution and then surfactant-rich oil can be supplies for formation of the droplet interface bilayer in the side well.

The need for the three-dimensional structures of the traps (i.e. continuous slope of the floor of storage wells) dictated the choice of

micromilling over the standard soft lithography methods. In addition, the chemical composition of continuous phase prevented us from using PDMS (which swells in the presence of hexadecane [35]) as a device material. The geometry of the chip presented in this study is fully compatible with mass production schemes, such as injection molding – for precise and faster reproduction [36–38]. Our system does not require complex actuation (e.g. valves, piezoelectric modules) neither optical sensors for feedback-triggered control of microflows of fluids [39–41]. It is rather based on the use of user friendly syringe pumps. The use of microfluidic methods is gaining popularity in biochemical and biophysical research, and the basic equipment for microfluidic experiments is being present in a growing number of laboratories. We also hope that in the future simpler sources of flow can be adopted for execution of operation on this passive system – e.g. a pipette [23], pumping lids [26] or passive pumping method [42,43].

We demonstrated the capability of measuring the passive permeation of small molecules through the lipid bilayers. Transport of fluorescein between droplets connected via lipid bilayer was shown as a proof of the correct formation of membranes, however rarely it was followed by the quantitative description of the process [11,21]. Droplets are a perfect tool to study transport phenomena, as they provide containers of well-defined volumes and, when immobilised in traps, result in a stable area of contact. It was previously proved that the investigated small molecule – fluorescein – does not leak from droplets into the surrounding hexadecane, thus, in view of that research, the transport through a lipid membrane is the only plausible route [11]. We calculated the permeability coefficient of fluorescein to be equal to  $5.39 \times 10^{-8}$  m/s in pH 7.3. This value is very close to the results shown by Nisisako et al. ( $5.1 \times 10^{-8}$  m/s in pH 7.5) [8]. Slightly higher value of permeability coefficient results from using lower pH (7.3 instead of 7.5) at which more species of fluorescein become uncharged and able to permeate. In addition the difference may result from the presence of silicone oil in continuous phase, which was reported to have a significant influence on bilayers structure and properties [27]. Interestingly the calculated permeability coefficient value through DOPC bilayer is very close to a value measured in an endothelial cells culture ( $5.8 \times 10^{-8}$  m/s) [44]. In spite of the establishment of precise electrophysiological methods which allow for single-channel measurements, the fluorescence imaging creates new possibilities in studying of the activity of membrane proteins. Monitoring the flux of ions associated with excitation of fluorescence is a non-invasive method, which can be easily automated for collection of data from parallel compartments. Moreover, the fluorescence read-out is usually more widely accessible among researchers than devices for electrophysiological recordings. However, the combination of both approaches and implementation of electrodes to the parallel dilution DIB system, recently shown by Nguyen et al. [32] and Taylor et al. [45], would open up additional avenues for quantification of transport of molecules.

As a biologically relevant demonstration, we have chosen to measure the ion flux through natural nanopores incorporated in the lipid bilayer. We chose  $\alpha$ -hemolysin protein for its predictable assembly into structurally well-defined channels passing small molecules through the membrane. The measurements of  $\text{Ca}^{2+}$  flow through  $\alpha$ HL nanopores confirmed the data from similar experiments conducted in non-microfluidic system by Castell et al. showing an increase of fluorescent dye sensitive to the presence of calcium ions [15]. Most studies so far focused on showing the transport through  $\alpha$ -hemolysin on a single-channel level [46,47]. Here we take a different approach. Based on the available literature data and by creating a model which allows us to calculate the permeability rates we estimate the number of nanopores present in the bilayer.

We generated droplets of reproducible volumes of  $8.7 \pm 0.5$  nL. The small volume of droplets and bilayers allows for collection of data in a reasonable period of time (ca. 60 min). For the sizes of droplets used in the original work presenting Meter&Store traps, the characteristic time for diffusion would be 447 s. Here, this time was reduced

to 33 s only, allowing for assumption of uniform distribution of molecules within the compartments for the purpose of data analysis. Smaller droplets are possible to obtain using different fabrication strategy e.g. multilayer soft lithography [48]. However, the acquisition of images of multiple points using motorized microscope cannot be done at once due to the limited imaging area. For 12 pairs of droplets it takes 30 s to acquire images of all of them. In addition, there is a variation between each pair of droplets in the exact moment of formation of bilayer. Differences at the level of few seconds do not significantly affect final results of experiments lasting ca. 60 min, but could be problematic in the case of very short experiments. Therefore, we did not aim to miniaturize the system to the further extend, due to the limitations in the rate of detection.

#### 4. Conclusions

We report a novel application of the significantly re-engineered microfluidic architecture – Meter&Store trap – for parallel generation of artificial lipid bilayers. The main innovation lies in the fact, that operations on samples are hard-wired in the structure of the microfluidic channels. As a result, the device does not require neither special equipment nor operator's expertise in microfluidics. Easy to operate syringe pumps are sufficient for preparation of nanoliter aqueous plugs and for generation of 12 functional lipid bilayers at the interface of droplets. We demonstrate the determination of permeation rate of small molecule (fluorescein) through the lipid bilayers. In addition, we quantify the activity of membrane protein ( $\alpha$ -hemolysin) based on optical detection of differences in calcium ion levels between the droplets. By taking the advantage of the construction of hydrodynamic traps comprising the device, we prepare various concentrations of  $\alpha$ HL. We show that the rate of transport depends on the number of protein molecules within the droplet.

#### Author contributions

M.A.C., T.S.K. and P.G. conceived and designed the experiments, M.A.C. and T.S.K. performed the experiments and analyzed the data, K.M. analyzed the data and developed mathematical models, M.A.C., T.S.K., K.M. and P.G. wrote the paper.

#### Conflict of interest

There are no conflicts of interest to declare.

#### Acknowledgements

The project is co-financed by the European Research Council Grant 279647. M.A.C. was supported by National Science Centre within the scholarship ETIUDA (decision number DEC-2017/24/T/ST4/00334). T.S.K. was supported by the Ministry of Science and Higher Education through the scholarship for outstanding young researchers (agreement 0722/E 64/STYP/10/295) and by National Science Centre within the scholarship ETIUDA (decision number DEC-2014/12/T/ST4/00649). K.M. was supported by National Science Centre, through Sonata 2016/21/D/ST3/00988 grant. M.A.C. and P.G. were partially financed by Symfonia2014/12/W/NZ6/00454 project funded by National Science Centre. This project was partially performed in the Ultrafast Microfluidic Devices Laboratory within the project NanoFun POIG.02.02.00-00-025/09 funded by Ministry of Regional Development, Ministry of Science and Higher Education and Innovative Economy Programme.

#### Appendix A. Supplementary data

Supplementary material related to this article can be found, in the online version, at doi:<https://doi.org/10.1016/j.snb.2019.01.143>.

## References

- [1] J. Dunlop, M. Bowlby, R. Peri, D. Vasilyev, R. Arias, High-throughput electrophysiology: an emerging paradigm for ion-channel screening and physiology, *Nat. Rev. Drug Discov.* 7 (2008) 358–368, <https://doi.org/10.1038/nrd2552>.
- [2] M. Takinoue, S. Takeuchi, Droplet microfluidics for the study of artificial cells, *Anal. Bioanal. Chem.* 400 (2011) 1705–1716, <https://doi.org/10.1007/s00216-011-4984-5>.
- [3] Z. Cournia, T.W. Allen, I. Andricioaei, B. Antonny, D. Baum, G. Brannigan, N.-V. Buchete, J.T. Deckman, L. Delemotte, C. del Val, R. Friedman, P. Gkeka, H.-C. Hege, J. Hénin, M.A. Kasimova, A. Kolocouris, M.L. Klein, S. Khalid, M.J. Lemieux, N. Lindow, M. Roy, J. Selent, M. Tarek, F. Tofoleanu, S. Vanni, S. Urban, D.J. Wales, J.C. Smith, A.-N. Bondar, Membrane protein structure, function and dynamics: a perspective from experiments and theory, *J. Membr. Biol.* 248 (2015) 611–640, <https://doi.org/10.1007/s00232-015-9802-0>.
- [4] T. Osaki, S. Takeuchi, Artificial cell membrane systems for biosensing applications, *Anal. Chem.* 89 (2017) 216–231, <https://doi.org/10.1021/acs.analchem.6b04744>.
- [5] K. Funakoshi, H. Suzuki, S. Takeuchi, Lipid bilayer formation by contacting monolayers in a microfluidic device for membrane protein analysis, *Anal. Chem.* 78 (2006) 8169–8174, <https://doi.org/10.1021/ac0613479>.
- [6] H. Bayley, E. Harth, B. Cronin, A. Heron, M.A. Holden, W.L. Hwang, R. Syeda, J. Thompson, M. Wallace, Droplet interface bilayers, *Mol. Biosyst.* 4 (2008) 1191–1208, <https://doi.org/10.1039/b808893d>.
- [7] M.J. Booth, V.R. Schild, H. Bayley, F.G. Downs, Functional aqueous droplet networks, *Mol. Biosyst.* 13 (2017) 1658–1691, <https://doi.org/10.1039/c7mb00192d>.
- [8] T. Nisisako, S. a Portonovo, J.J. Schmidt, Microfluidic passive permeability assay using nanoliter droplet interface lipid bilayers, *Analyst* 138 (2013) 6793–6800, <https://doi.org/10.1039/c3an01314f>.
- [9] P.H. King, G. Jones, H. Morgan, M.R.R. de Planque, K.-P. Zauner, Interdroplet bilayer arrays in millifluidic droplet traps from 3D-printed moulds, *Lab Chip* 14 (2014) 722–729, <https://doi.org/10.1039/C3LC51072G>.
- [10] Y. Elani, A. Gee, R.V. Law, O. Ces, Engineering multi-compartment vesicle networks, *Chem. Sci.* 4 (2013) 3332–3338, <https://doi.org/10.1039/C3SC51164B>.
- [11] C.E. Stanley, K.S. Elvira, X.Z. Niu, A.D. Gee, O. Ces, J.B. Edel, A.J. Demello, A microfluidic approach for high-throughput droplet interface bilayer (DIB) formation, *Chem. Commun.* 46 (2010) 1620–1622, <https://doi.org/10.1039/b924897h>.
- [12] Y. Elani, X.C.I. Solvas, J.B. Edel, V. Law, O. Ces, Microfluidic generation of encapsulated droplet interface bilayer networks (multisomes) and their use as cell-like reactors, *Chem. Commun.* 52 (2016) 5961–5964, <https://doi.org/10.1039/c6cc01434h>.
- [13] N.E. Barlow, G. Bolognesi, A.J. Flemming, N.J. Brooks, M.C. Barter, O. Ces, Lab on a chip multiplexed droplet interface bilayer formation, *Lab Chip* (2016) 4653–4657, <https://doi.org/10.1039/c6lc01011c>.
- [14] S. Ota, H. Suzuki, S. Takeuchi, Microfluidic lipid membrane formation on micro-chamber arrays, *Lab Chip* 11 (2011) 2485–2487, <https://doi.org/10.1039/C1LC20334G>.
- [15] O.K. Castell, J. Berridge, M.I. Wallace, Quantification of membrane protein inhibition by optical ion flux in a droplet interface bilayer array, *Angew. Chem. — Int. Ed.* 51 (2012) 3134–3138, <https://doi.org/10.1002/anie.201107343>.
- [16] T. Tonooka, K. Sato, T. Osaki, R. Kawano, S. Takeuchi, Lipid bilayers on a picoliter microdroplet array for rapid fluorescence detection of membrane transport, *Small* 10 (2014) 3275–3282, <https://doi.org/10.1002/sml.201303332>.
- [17] I. Kusters, A.M. van Oijen, A.J.M. Driessen, Membrane-on-a-chip: microstructured silicon/silicon-dioxide chips for high-throughput screening of membrane transport and viral membrane fusion, *ACS Nano* 8 (2014) 3380–3392, <https://doi.org/10.1021/nn405884a>.
- [18] M. Urban, A. Kleefen, N. Mukherjee, P. Seelheim, B. Windschiegel, M. Vor der Brüggen, A. Koçer, R. Tampé, Highly parallel transport recordings on a membrane-on-nanopore chip at single molecule resolution, *Nano Lett.* 14 (2014) 1674–1680, <https://doi.org/10.1021/nl5002873>.
- [19] N. Soga, R. Watanabe, H. Noji, Attolitre-sized lipid bilayer chamber array for rapid detection of single transporters, *Sci. Rep.* 5 (2015) 11025.
- [20] R. Watanabe, N. Soga, T. Yamanaka, H. Noji, High-throughput formation of lipid bilayer membrane arrays with an asymmetric lipid composition, *Sci. Rep.* 4 (2014) 7076, <https://doi.org/10.1038/srep07076>.
- [21] B. Schlicht, M. Zagnoni, Droplet-interface-bilayer assays in microfluidic passive networks, *Sci. Rep.* 5 (2015) 9951, <https://doi.org/10.1038/srep09951>.
- [22] T.S. Kaminski, P. Garstecki, Controlled droplet microfluidic systems for multistep chemical and biological assays, *Chem. Soc. Rev.* 46 (2017) 6210–6226, <https://doi.org/10.1039/c5cs00717h>.
- [23] L. Derzsi, T.S. Kaminski, P. Garstecki, Antibigrams in five pipetting steps: precise dilution assays in sub microliter volumes with a conventional pipette, *Lab Chip* 16 (2016) 893–901, <https://doi.org/10.1039/C5LC01151E>.
- [24] S.A. Rani, B. Pitts, P.S. Stewart, Rapid diffusion of fluorescent tracers into staphylococcus epidermidis biofilms visualized by time lapse microscopy, *Antimicrob. Agents Chemother.* 49 (2005) 728–732 <http://aac.asm.org/content/49/2/728.abstract>.
- [25] J. Guzowski, P.M. Korczyk, S. Jakiela, P. Garstecki, Automated high-throughput generation of droplets, *Lab Chip* 11 (2011) 3593, <https://doi.org/10.1039/c1lc20595a>.
- [26] S. Begolo, D.V. Zhukov, D.A. Selck, L. Li, R.F. Ismagilov, The pumping lid: investigating multi-material 3D printing for equipment-free, programmable generation of positive and negative pressures for microfluidic applications, *Lab Chip* 14 (2014) 4616–4628, <https://doi.org/10.1039/C4LC00910J>.
- [27] G.J. Taylor, G.A. Venkatesan, C.P. Collier, S.A. Sarles, Direct in situ measurement of specific capacitance, monolayer tension, and bilayer tension in a droplet interface bilayer, *Soft Matter* 11 (2015) 7592–7605, <https://doi.org/10.1039/C5SM01005E>.
- [28] K. Leung, H. Zahn, T. Leaver, K.M. Konwar, N.W. Hanson, A.P. Pagé, C.-C. Lo, P.S. Chain, S.J. Hallam, C.L. Hansen, A programmable droplet-based microfluidic device applied to multiparameter analysis of single microbes and microbial communities, *Proc. Natl. Acad. Sci. U. S. A.* 109 (2012) 7665, <https://doi.org/10.1073/pnas.1106752109>.
- [29] L. Mazutis, A.D. Griffiths, Selective droplet coalescence using microfluidic systems, *Lab Chip* 12 (2012) 1800–1806, <https://doi.org/10.1039/C2LC40121E>.
- [30] M. Lee, J.W. Collins, D.M. Aubrecht, R.A. Sperling, L. Solomon, J.-W. Ha, G.-R. Yi, D. Weitz, V.N. Manoharan, Synchronized reinjection and coalescence of droplets in microfluidics, *Lab Chip* 14 (2014) 509–513, <https://doi.org/10.1039/C3LC51214B>.
- [31] P. Carreras, Y. Elani, R.V. Law, N.J. Brooks, J.M. Seddon, O. Ces, A microfluidic platform for size-dependent generation of droplet interface bilayer networks on rails, *Biomicrofluidics* 9 (2015) 0–7, <https://doi.org/10.1063/1.4938731>.
- [32] M.-A. Nguyen, B. Srijanto, C.P. Collier, S.T. Retterer, S.A. Sarles, Hydrodynamic trapping for rapid assembly and in situ electrical characterization of droplet interface bilayer arrays, *Lab Chip* 16 (2016) 3576–3588, <https://doi.org/10.1039/C6LC00810K>.
- [33] Y. Bai, X. He, D. Liu, S.N. Patil, D. Bratton, A. Huebner, F. Hollfelder, C. Abell, W.T.S. Huck, A double droplet trap system for studying mass transport across a droplet-droplet interface, *Lab Chip* 10 (2010) 1281–1285, <https://doi.org/10.1039/b925133b>.
- [34] N. Bremond, A.R. Thiam, Decompressing emulsion droplets favors coalescence, *Phys. Rev. Lett.* 24501 (2008) 1–4, <https://doi.org/10.1103/PhysRevLett.100.024501>.
- [35] R. Dangla, F. Gallaire, C.N. Baroud, Microchannel deformations due to solvent-induced PDMS swelling, *Lab Chip* 10 (2010) 2972–2978, <https://doi.org/10.1039/c003504a>.
- [36] U.N. Lee, X. Su, D.J. Guckenberger, A.M. Dostie, T. Zhang, E. Berthier, A.B. Theberge, Fundamentals of rapid injection molding for microfluidic cell-based assays, *Lab Chip* 18 (2018) 496–504, <https://doi.org/10.1039/C7LC01052D>.
- [37] C.W. Kan, A.J. Rivnak, T.G. Campbell, T. Piech, D.M. Rissin, M. Mosl, A. Peterca, H.-P. Niederberger, K.A. Minnehan, P.P. Patel, E.P. Ferrell, L.E. Meyer, L. Chang, D.H. Wilson, D.R. Fournier, D.C. Duffy, Isolation and detection of single molecules on paramagnetic beads using sequential fluid flows in microfabricated polymer array assemblies, *Lab Chip* 12 (2012) 977–985, <https://doi.org/10.1039/C2LC20744C>.
- [38] B.J. Hindson, K.D. Ness, D.A. Masquelier, P. Belgrader, N.J. Heredia, A.J. Makarewicz, L.J. Bright, M.Y. Lucero, A.L. Hiddessen, T.C. Legler, T.K. Kitano, M.R. Hodel, J.F. Petersen, P.W. Wyatt, E.R. Steenblock, P.H. Shah, L.J. Bousse, C.B. Troup, J.C. Mellen, D.K. Wittmann, N.G. Erndt, T.H. Cauley, R.T. Koehler, A.P. So, S. Dube, K.A. Rose, L. Montesclaros, S. Wang, D.P. Stumbo, S.P. Hodges, S. Romine, F.P. Milanovich, H.E. White, J.F. Regan, G.A. Karlin-Neumann, C.M. Hindson, S. Saxonov, B.W. Colston, High-throughput droplet digital PCR system for absolute quantitation of DNA copy number, *Anal. Chem.* 83 (2011) 8604–8610, <https://doi.org/10.1021/ac202028g>.
- [39] M.A. Czekalska, T.S. Kaminski, S. Jakiela, K.T. Sapra, H. Bayley, P. Garstecki, A droplet microfluidic system for sequential generation of lipid bilayers and transmembrane electrical recordings, *Lab Chip* 15 (2015) 541–548, <https://doi.org/10.1039/c4lc00985a>.
- [40] D. Wong, C.L. Ren, Microfluidic droplet trapping, splitting and merging with feedback controls and state space modelling, *Lab Chip* 16 (2016) 3317–3329, <https://doi.org/10.1039/C6LC00626D>.
- [41] M.A. Czekalska, S.T. Kaminski, M. Horka, S. Jakiela, P. Garstecki, An automated microfluidic system for the generation of droplet interface bilayer networks, *Micromachines* 8 (2017), <https://doi.org/10.3390/mi8030093>.
- [42] S.C. Saha, A.J. Henderson, A.M. Powl, B.A. Wallace, M.R.R. de Planque, H. Morgan, Characterization of the prokaryotic sodium channel Navsp pore with a microfluidic bilayer platform, *PLoS One* 10 (2015) e0131286, <https://doi.org/10.1371/journal.pone.0131286>.
- [43] G.M. Walker, D.J. Beebe, A passive pumping method for microfluidic devices, *Lab Chip* 2 (2002) 131–134, <https://doi.org/10.1039/B204381E>.
- [44] M. Simon, W.H. Kang, S. Gao, S. BAnta, B. Morrison III, TAT is not capable of transcellular delivery across an intact endothelial monolayer in vitro, *Ann. Biomed. Eng.* 39 (2011) 394–401, <https://doi.org/10.1007/s10439-010-0144-x>.
- [45] G. Taylor, M. Nguyen, S. Koner, E. Freeman, C.P. Collier, S.A. Sarles, Electrophysiological interrogation of asymmetric droplet interface bilayers reveals surface-bound alamethicin induces lipid flip-flop, *Biochim. Biophys. Acta (BBA) – Biomembr.* 1 (2019) 335–343.
- [46] A.J. Heron, J.R. Thompson, B. Cronin, H. Bayley, M.I. Wallace, Simultaneous measurement of ionic current and fluorescence from single protein pores, *J. Am. Chem. Soc.* (2009) 1652–1653.
- [47] R. Watanabe, N. Soga, D. Fujita, K.V. Tabata, L. Yamauchi, S.H. Kim, D. Asanuma, M. Kamiya, Y. Urano, H. Suga, H. Noji, Molecule analysis of membrane transporter activity, *Nat. Commun.* 5 (2014) 1–8, <https://doi.org/10.1038/ncomms5519>.
- [48] H.-H. Jeong, B. Lee, S.H. Jin, S.-G. Jeong, C.-S. Lee, A highly addressable static droplet array enabling digital control of a single droplet at pico-volume resolution, *Lab Chip* 16 (2016) 1698–1707, <https://doi.org/10.1039/C6LC00212A>.

Magdalena Czekalska received her MSc in Biotechnology from Warsaw University of Life Sciences in 2013. Since then, she is a PhD candidate in prof. Piotr Garstecki group at the Institute of Physical Chemistry of the Polish Academy of Sciences in Warsaw. Her research interests include the use of microfluidic techniques for studying protein-lipid interactions. She has conducted her research projects in collaboration with prof. Hagan

Bayley's group from Oxford University, and currently is a visiting student to prof. Tuomas Knowles group at Cambridge University, UK.

**Tomasz Kaminski** is a Marie Skłodowska-Curie postdoctoral researcher in the group of prof. Hollfelder at the Biochemistry Department of the University of Cambridge. Prior to coming to Cambridge he completed graduate studies in physical chemistry and a short postdoctoral stay in the group of prof. Piotr Garstecki at the Institute of Physical Chemistry of the Polish Academy of Sciences in Warsaw. During PhD studies he has been involved in the development of new micro-droplet technologies to a range of challenges in microbiology and biochemistry. He co-authored 18 publications and 21 patents and patent applications. He has conducted his research projects in collaboration with foreign research groups from Oxford University, University of Wisconsin-Madison, University of Tokyo and with spin-off companies from the laboratory led by prof. Garstecki.

**Karol Makuch** is an Assistant Professor at the Institute of Physical Chemistry of the Polish

Academy of Sciences and works in the microfluidic group of prof. Piotr Garstecki. He obtained MSc in 2005 and PhD in 2011 in theoretical physics from the University of Warsaw where he also served as a postdoctoral fellow until 2015 working on quantum condensed matter. In 2015 he joined prof. Piotr Garstecki group and in 2017 he was a postdoctoral researcher in prof. John Brady group at the California Institute of Technology.

**Piotr Garstecki** is a Full Professor at the Institute of Physical Chemistry of the Polish Academy of Science, where he leads the Microfluidics and Complex Fluids Research Group. He obtained MSc in Theoretical Physics from the College of Science in 1998 and PhD in Chemistry from the Institute of Physical Chemistry PAS. He later served as a postdoctoral fellow in the group of Prof. George Whitesides at Harvard University. He coauthored over a hundred scientific publications and multiple patent applications and cofounded multiple spin-out companies that use microfluidic technologies for the development of medical diagnostic systems.